Numerical Study of an Under-Expanded Jet

B. J. Gribben[1]
1 Crocodile Clips Ltd, Queensferry Street Lane, Edinburgh EH2 4PF, United Kingdom,
Brian.Gribben@crocodile-clips.com

Abstract

The use of a numerical method to examine the flow in the nozzle and plume of a low density under-expanded jet is described. Under-expanded jets are found in a number of applications, for example rocket exhausts at high altitude, vehicle manoeuvring thrusters, propulsion simulation devices and fuel injectors. The flow is characterised by a complex flow-field with a sudden expansion of the free jet from the nozzle, compression wave reflection at the jet boundary and shock wave reflection at the plume axis, resulting in a repeated 'barrel shock' pattern. Confidence in the numerical results is established by comparison with experimental data from the Low Density Tunnel at Qinetiq (formerly DERA Farnborough). The high resolution of the numerical results has contributed to the understanding of several flow features: shock reflection hysteresis; Mach disc curvature; flow stagnation and recirculation behing the Mach disc; the presence of a small diameter Mach disc in the apparent regular reflection. The potential of a numerical approach to complex nozzle/plume problems of this nature is discussed.

Introduction

Complex physical phenomena can occur in the vicinity of the nozzle outlets of launcher vehicles. The modelling of shock interaction, heat transfer, post-burning etc. are all of practical importance, so the accurate prediction of nozzle, afterbody and plume flow features are important to designers. Both over- and under-expanded jets can give rise to complex shock interactions. In an over-expanded nozzle, separation may take place inside the nozzle, having important consequences for propulsive efficiency and heat transfer. The plumes of under-expanded jets are characterised by strong expansions at the nozzle lip. The plume cross-sectional area increases sharply, producing an obstacle effect to the main flow. This in turn creates a shock wave emanating from the base corner or immediately upstream, which may separate the flow on the aft part of the fuselage. Separated flow in this area can lead to loss of control surface effectiveness, to hot exhaust gases coming into contact with the fuselage surface, and stability problems due to separation unsteadiness and/or asymmetry. For multi-nozzle launch vehicles the interaction

of the jet plumes adds to the complexity of the patterns. Recirculating exhaust gas can cause areas of high heat transfer at the base.

The experimental studies of Crist [1] and Abbett [2] established the basic wave structure of a highly underexpanded jet plume and that regular or Mach shock reflection may occur depending on the conditions. The method of characteristics has been employed by many authors [2], [3], [4], [5] in an attempt to develop predictive models for the core expansion and Mach disc location. Axisymmetric Euler and Navier-Stokes solvers have been used to obtain numerical solutions for underexpanded jet plumes with impressive results, see for example [6], [7], [8], [9]. These calculations demonstrate good agreement with experiment for a wide range of conditions using parameters such as Mach disc location and centreline velocity and are reported to capture the complex wave structure in detail.

The focus of this work is to examine a hysteresis phenomenon in a highly underexpanded jet.The existence of a hysteresis effect in the type of reflection of a two-dimensional oblique shock wave at a wall or symmetric line has been established in recent years. The reflection of the oblique shock wave may take the form of a regular reflection (RR) or Mach reflection (MR). The type of reflection which occurs depends on the Mach number upstream of the incident shock and the shock angle. However, there is a dual solution domain where either type may occur and the solution exhibits a hysteresis effect. For an overview of shock reflection hysteresis in the context of two-dimensional uniform flow see for example [10], [11]. The occurrence of a hysteresis effect in the shock reflection type of a highly underexpanded jet has been observed by Welsh[12]. In this work an established, general purpose flow solver will be applied to the same case and the experimental and numerical results compared.

Experimental Method

The experimental method is outlined here. The experiments were performed by F.P. Welsh at Qinetiq Farnborough and are fully described elsewhere [12]. The Low Density Tunnel was used to generate large ($\sim$300mm first shock cell length) plumes for probing with a non-intrusive electron beam fluorescence system. A hysteresis was observed in the shock reflection type of an under-expanded jet issuing from a nominally Mach 3 supersonic nozzle. Data was acquired for rotational temperature, density, static pressure and entropy change. The data reduction scheme for rotational temperature utilised an empirical approach based upon calibration measurements of the multi-quantum transition probabilities for the electron collision induced excitation of the nitrogen molecules. The integrated intensity of the fluorescence signal was used to measure the local gas density. Electron beam fluorescence was also used to obtain flow visualisation photographs.

Numerical Method

Flow Solver

A general purpose, two-dimensional or axisymmetric Navier-Stokes flow solver is used. The main features of the method used are outlined here, for details see references [13]. A multi-

block structured, cell-centred, finite volume method is employed. Osher's scheme and MUSCL variable interpolation are used to discretise the convective terms and central differencing for the diffusive terms. The linear system arising at each implicit time step is solved using a Generalised Conjugate Gradient method. A Block Incomplete Lower-Upper (BILU) factorisation is used as a preconditioner. An important feature of the flow solver is the use of approximate Jacobian matrices for the left hand side of the linear system. This has led to substantial reductions in memory and CPU-time requirements compared to the use of exact Jacobians.

For this study it is assumed throughout that the working gas is in the continuum regime with no condensation and has constant specific heats. These assumptions have been verified[14] and are confirmed by the Hypersonic Aerodynamics Group where the shock reflection experiments were carried out.

Boundary Conditions

Figure 1 shows a diagram of the computational domain for the nozzle/plume calculations with labelled boundary condition types (the size of the nozzle is exaggerated for clarity). At the boundary labelled A an adiabatic wall boundary condition, with no slip and zero normal pressure gradient, was applied. At B a symmetry condition was applied. At C the flow variables were extrapolated from the interior of the domain except for the case of locally subsonic outflow where pressure is imposed at the background level.

At D it is assumed that the total enthalpy and entropy are the same for the reservoir r and nozzle inlet i, thus obtaining expressions for the pressure p_i and density ρ_i which are imposed. The velocity components are extrapolated from the interior of the domain. Note that assuming constant entropy s implies a constant entropy measure S defined by

$$S = \frac{p}{\rho^\gamma}$$

where γ is the ratio of specific heats. For convenience the non-dimensionalisation is constructed such that

$$\rho_r = 1, \qquad p_r = \frac{1}{\gamma} \tag{1}$$

are the values of density and pressure respectively in the reservoir. The reservoir sound speed, total enthalpy and the entropy measure are then

$$a_r = 1, \qquad H_r = \frac{1}{(\gamma - 1)}, \qquad S_r = \frac{1}{\gamma}$$

We now have two conditions to impose at the inlet i :

$$H_r = \frac{\gamma p_i}{(\gamma - 1)\,\rho_i} + \frac{u_i^2 + v_i^2}{2}, \qquad S_r = \frac{p_i}{\rho_i^\gamma}$$

The velocity components u_i and v_i are extrapolated from the interior of the domain. The inlet density and pressure are then

$$\rho_i = \left[1 - \frac{u_i^2 + v_i^2}{2}\,(\gamma - 1))\right], \qquad p_i = \frac{1}{\gamma}\rho_i^\gamma$$

For the boundary condition treatment at E the background stagnation conditions are known but the flow direction is not known $a\ priori$. This being similar to the nozzle inlet boundary treament, the boundary conditions here are treated in the same manner except that background conditions are used instead of reservoir conditions in equations (1).

For the simpler nozzle only calculations, the boundary conditions at A,B,D are applied as described above, and at the nozzle outlet the flow variables were extrapolated.

Initial Conditions and Pseudo-Steady Approach

As a first step to studying the full problem a preliminary calculation for the nozzle only was carried out. Using a linear variation from reservoir to Mach 3 conditions along the axis from the inlet to the outlet as initial conditions was found to considerably reduce the calculation time compared with using uniform reservoir or sonic conditions. The solution from this calculation was used as the initial solution in the nozzle for the main calculation, where the calculated nozzle exit conditions were used as the initial conditions for the domain directly downstream of the nozzle exit. For the remainder of the domain the background conditions were applied as initial conditions. Calculations were performed over a range of pressure ratios from well inside the regular reflection range to well inside the Mach reflection range including the hysteresis loop. A quasi-steady approach was employed in order to account for time history effects. First, converged solutions were obtained for the conditions at the extremities of the range of interest. These were used as initial solutions for a calculation with a small change in pressure ratio, thus beginning to traverse the range, this solution being used subsequently as the next initial solution and so on. By using a small step change in pressure ratio between calculations this approach is very robust and converges quickly at each condition. A reduction of just over two orders of magnitude in the residual was found to be sufficient for the step size used. This usually required around 100 steps to achieve but may require up to 500 steps when a switch in shock reflection type occurs. By contrast, obtaining a converged solution (without the aid of a close initial solution) for the end points of the pressure ratio range is far more demanding, requiring approximately 30 times the computational effort. The step change in pressure ratio used is 2.857, corresponding to a step change in reservoir stagnation pressure of 0.1 $torr$ for a background pressure of 35 $mtorr$ in terms of the original experiments.

Grid

The grid generation for this case is straightforward due to the simple geometry. The computational domain extends 70 nozzle throat diameters downstream in order to capture at least two shock cells and 20 diameters radially from the symmetric line. The grid within the nozzle consists of 58 and 21 points in the axial and radial directions respectively, this number having been determined from a grid convergence study carried out independently of the plume calculations. The plume calculations were also performed using a number of grids. A grid convergence study was carried out using the criterion of the calculated limits of the hysteresis loop. A grid converged solution was obtained using 937 and 65 points in the axial and radial directions respectively [14]. For any given pressure ratio the grid is excessively fine in places, but since the location of the shock reflections vary widely with pressure ratio and the same grid was used in each case this was unavoidable.

Mach 3 Nozzle

Welsh[12] describes a series of experiments where the effect of varying the ratio of reservoir stagnation pressure p_r to background pressure p_b on the plume of a highly under-expanded nitrogen jet is examined. The reported shock reflection hysteresis phenomenon provided the motivation for this CFD study. In the experiments p_r was varied and p_b was kept constant. In this way the nozzle exit conditions as well as the pressure ratio were varied. In addition, experiments were carried out for a number of values of p_b and for two different nozzle sizes. It is difficult then to isolate the effect of the varying pressure ratio. For these reasons, as a preliminary to the nozzle-plume study, it is useful to perform calculations for the nozzle alone in order to examine the effect of the nozzle Reynolds number on the nozzle exit conditions. This will help to put subsequent nozzle-plume calculations and comparison with experiment in their proper context.

Calculations were performed for a range of reservoir stagnation pressures, from 2 $torr$ to 70 $torr$, covering the range used in the experiments. The grid within the nozzle consists of 58 and 21 points in the axial and radial directions respectively, this number having been determined from a grid convergence study carried out independently of the plume calculations. The reservoir stagnation temperature T_o is constant at 288.0K and the two throat diameters used are 5.19 mm and 15.3 mm. The Reynolds number based on throat conditions Re can then be calculated for each p_r, assuming sonic conditions at the throat, using the isentropic relations and Sutherland's law for viscosity. The variation of Re with pressure ratio for each nozzle is shown in Figure 2(a). The present CFD method was then used to obtain results for the nozzle flow for a range of Re.

The calculated variation of the maximum nozzle exit Mach no. M_{exit} with throat Reynolds number Re is shown in Figure 2(b). The crosses in the figure, which have been joined by straight lines, indicate the twenty calculation points. Calculated pressure contours for Re= 800 are shown in Figure 3(a). As expected, as Re decreases so does M_{exit}, caused by the displacement effect of the boundary layer decreasing the effective area of the divergent section of the nozzle. The thickness of the boundary layer can be visualised from the Mach number plot Figure 3(b). The magnitude of the trend confirms that for each of the experiments the nozzle exit conditions vary significantly.

Under-Expanded Jet

Shock Reflection Hysteresis

The shock reflection hysteresis phenomenon observed in a series of low density, under-expanded jet experiments by Welsh[12] provides the motivation for this study. The jet plume is characterised by complex shock and expansion wave interactions. Although state of the art non-intrusive measurement techniques were employed to good effect in the experiments, the high resolution of a numerical study could potentially greatly enhance the understanding of the plume structures. The approach adopted is to use the available experimental data and flow visualisa-

tions to establish confidence in the CFD results, then to use the CFD results to examine the flow features of interest.

The nozzle calculations described above, covering the experimental range of conditions as a preliminary to this main study, confirmed that a varying reservoir stagnation pressure has a significant effect on the nozzle exit conditions. With this in mind, the present calculations were performed with a constant nozzle throat Reynolds number Re of 4000 (implying a constant reservoir stagnation pressure) and a varying background pressure. In this way the nozzle exit conditions are constant enabling examination of the pressure ratio influence independently. Comparison will be made here with the experimental conditions where the value of Re in the reported dual solution domain is closest to our constant value, namely the case with D=15mm, p_b=35mtorr where the value of Re varies between approximately 3500 and 4500 in the dual solution domain. The nozzle solution provided initial conditions for the full problem. Calculations were performed over a range of pressure ratios from well inside the regular reflection range to well inside the Mach reflection range including the hysteresis loop. The quasi-steady approach described above was employed in order to account for time history effects.

The calculated shock reflection type and distance variation with pressure ratio is shown in Figure 4. The shock reflection distance is the axial distance (X_{sr}) from the nozzle exit to the centre of the first centre-line regular reflection or Mach disc, non-dimensionalised with respect to the nozzle throat diameter. The figure shows how for a small range of pressure ratios either regular reflection (RR) or Mach reflection (MR) may occur. Which condition prevails depends on the time history of the plume development, in accordance with experimental observation. Selecting, for example, the pressure ratio value of 300 in Figure 4, the corresponding point on the RR(MR) curve will be reached if the condition immediately prior was also on the RR(MR) curve. The arrows on the figure indicate the "flip" in reflection type which occurs at the limits of the hysteresis loop. From this figure it can be concluded that the quasi-steady approach has been successful, at least qualitatively, in modelling the shock reflection hysteresis phenomenon. Included in Figure 4 is the location of the hysteresis loop for the experimental conditions closest to the constant Reynolds number employed in the calculation. The experimental uncertainty of the shock reflection length corresponds to ± 0.33 of the non-dimensional length units used in the figure. Given the varying Reynolds number used in the experiment we cannot expect very close agreement between the CFD and experimental results and the agreement shown here is considered reasonable. In the case of two dimensional shock reflection hysteresis the limits of the dual solution domain can be calculated from knowledge of the Mach number upstream of the reflection and the incident shock angle[14, 10, 11]. In principle a similar analysis is possible here; the Mach number and local shock angle can be obtained from the CFD results, and the theoretical limits to the dual solution domain calculated and compared with the numerical results. However, this approach was not successful since the shock angles are difficult to measure to the necessary degree of accuracy from the field plots due to curvature of the shock and shock smearing.

Across most of the pressure ratio range the predicted reflection type matches the experimentally observed type. Very good agreement between calculated and experimental temperature profiles was achieved in these cases. Figures 5(a) and 5(b) show typical centre-line temperature comparisons. Note that absolute temperatures are shown here, the ambient temperature being 288K. In both figures the CFD results are for $Re = 4000$. In Figures 5(a) and 5(b) the experimental results are for $Re = 2522$ and 3625 respectively. The experimental data[12] was obtained using a non-intrusive measurement technique, with expected accuracy of $\pm 5\%$. The figures show a

good prediction of the shock reflection locations, RR and MR respectively, indicated by the sharp rise in temperature. Temperature comparisons across the plume (not shown here) also show good agreement.

Figures 6(a) and 6(b) show calculated density contours for both RR and MR for the same pressure ratio (p_r/p_b =285.7), a condition which lies in the dual solution domain. Note that upstream of the first shock reflection no difference in the flow behaviour can be detected, in accordance with experimental observations. The calculated centre-line distributions of all flow variables are identical upstream of the first shock reflection. It is also clearly shown in these figures that the MR occurs slightly upstream of the corresponding RR, allowing a greater initial expansion in the RR case. The field plots of the calculated results are in very good agreement with the flow visualisation photographs from the original experiments[12].

The grid convergence study and good agreement obtained, for both shock reflection distance and temperature values, over a range of pressure ratios and at several different axial stations, gives confidence in the accuracy of the calculations. The detail obtained from the CFD study was then used to examine a number of flow features.

Plume Structure

Figures 6(a) and 6(b) clearly show the repeated shock cell pattern, described in detail in reference [14], associated with an under-expanded jet. The shock reflection is the mechanism through which the condition of axial flow on the centre-line is achieved. Centre-line plots of pressure show that upstream of the first shock interaction the initial expansion along the axis of the plume is invariant with pressure ratio, and that before each shock reflection, the gas becomes significantly over-expanded.

The Mach reflection pattern is associated with higher pressure ratios. A recirculation zone was predicted behind the Mach disc, see Figure 7(a). This surprising feature has been previously noted in an as yet unpublished CFD study[12]. The recirculation is predicted in the present results for all the pressure ratios examined in the MR range. At the lower limit of the hysteresis loop (p_r/p_b = 217.1) the subsonic region is 5.58 throat diameters in length. At the highest pressure ratio considered (p_r/p_b = 685.7) the subsonic region is 8.82 throat diameters in length. Figure 7(b) shows centre-line pressure distributions for three pressure ratios at MR conditions. As can be seen from the figure, immediately downstream of the Mach disc the pressure is still increasing, this pressure gradient appearing to drive the recirculation. It is noted that the initial compression caused by the Mach disc brings the over-expanded gas up to ambient pressure. An explanation for the continuing increase in pressure is that immediately downstream of the Mach disc the gas being processed by the reflected oblique shock is of relatively high density due to the accumulation in the incident shock layer.

The calculated Mach disc is curved, convex if viewed from upstream, for each of the pressure ratio values examined. This feature can be detected in Figure 6(b). The amount of curvature increases slowly with pressure ratio, and implies that the flow is being turned away from the axis at the triple point. This corresponds to an Inverted Mach Reflection following Hornung's classification[10]. However, due to the curvature of all three shocks and their apparent thickness in the present results it is difficult to precisely identify the location of the triple point and verify the Mach Reflection type. The flow direction changes significantly in the locality of the triple

point, see Figure 7(a).

There is some evidence to suggest that the apparently regular reflections are in fact Mach reflections with a Mach disc of small diameter. In Figure 6(a) there appears to be a slip line behind the 'regular' reflection; compare with the slip line behind the Mach reflection in Figure 6(b). There is a significant subsonic region behind the 'regular' reflections at the higher pressure ratios. On close examination of the pressure contours in the region around the reflection there is an apparent Mach disc of approximately three grid cells in radius. Refinement of the grid in this area by a factor of ten had no impact on this feature. It appears that two different levels of Mach reflection are occurring. The incident shock waves to the reflection are curved, and conditions upstream of the shock are varying along the shock; a conventional pressure-deflection diagram approach borrowed from 2-D shock reflection analysis indicates the possibility of multiple Mach reflection solutions[14]. In addition, there is experimental and numerical evidence to suggest that a true axisymmetric regular reflection cannot exist, and what has previously been accepted as a regular reflection is in fact a very small diameter Mach reflection[12, 15]. This very small diameter Mach reflection has been termed an apparent regular reflection.

Conclusion

The hysteresis effect in underexpanded jet plumes reported by Welsh [12] has been successfully predicted using a CFD method. The good agreement with experimental results established confidence in the numerical approach. The value of the CFD analysis has been demonstrated in the detail that has been obtained from the results, enabling the examination and interpretation of flow features not initially recognised or fully understood from the experimental study alone.

Acknowledgements

Many thanks to Paul Welsh for generously providing the experimental data and helpful advice.

This work was supported by a University of Glasgow scholarship and sponsorship from DERA Bedford.

References

[1] C. Crist, P.M. Sherman and D.R. Glass "Study of the Highly Underexpanded Sonic Jet" AIAA Journal, vol 4, no. 1, pp 68-71, 1966.

[2] M. Abbett "Mach Disk in Underexpanded Exhaust Plumes" AIAA Journal, vol 9, no. 3, pp 512-514, 1971.

[3] J.H. Fox "On the Structure of Jet Plumes" AIAA Journal, vol 12, no. 1, pp 105-107, 1974.

[4] I.S. Chang and W.L. Chow "Mach Disk from Underexpanded Axisymmetric Nozzle Flow" AIAA Journal, vol 12, no. 8, pp 1079-1082, 1974.

[5] D.W. Eastman and L.P. Radtke "Location of the Normal Shock Wave on the Exhaust Plume of a Jet" AIAA Journal, vol 1, no. 4, pp 918-919, 1963.

[6] S.M. Prudhomme, and H. Haj-Hariri "Investigation of Supersonic Underexpanded Jets using Adaptive Unstructured Finite Elements" Finite Elements in Analysis and Design, vol 17, pp 21-40, 1994.

[7] P.S. Cumber, M. Fairweather, S.A.E.G. Falle and J.R. Giddings "Predictions of the Structure of Turbulent, Highly Underexpanded Jets" Journal of Fluids Engineering, vol 117, pp 599-604, Dec 1995.

[8] A.T. Hsu and M.S. Liou "Computational Analysis of Underexpanded Jets in the Hypersonic Regime" Journal of Propulsion and Power, vol 7, no. 2, pp 297-299, 1991.

[9] P. Birkby, J.C. Dent and G.J. Page "CFD prediction of Turbulent Sonic Underexpanded Jets" Proceedings of the 1996 ASME Fluids Engineering Summer Meeting. Part 2 (of 3), pp 465-470, 1996.

[10] H.G. Hornung "Regular and Mach Reflection of Shock Waves" Annual Review of Fluid Mechanics, vol 18, pp 33-58, 1986.

[11] G. Ben-Dor "Steady, Pseudo-Steady and Unsteady Shock Wave Reflections" Progress in Aerospace Sciences, vol 25, pp 329-412, 1988.

[12] F.P. Welsh "Electron beam fluorescence measurements of shock reflection hysteresis in an underexpanded jet" 21st International Symposium on Shock Waves, Great Keppel, Australia, 1997.

[13] Badcock, K.J., Richards, B.E. and Woodgate, M.A. Elements of Computational Fluid Dynamics on block structured grids using implicit solvers Progress in Aerospace Sciences, vol 36, pp 351-392, 2000.

[14] Gribben, B.J. and Badcock, K.J. and Richards, B.E. "Shock Reflection Hysteresis in an Underexpanded Jet: a CFD Study" University of Glasgow, Aero Report 9808, 1998.

[15] S. Molder, A. Gulamhussein, E.V. Timofeev and P.A. Voinovich "Focusing of conical shocks at the centre-line of symmetry" 21st International Symposium on Shock Waves, Great Keppel, Australia, 1997.

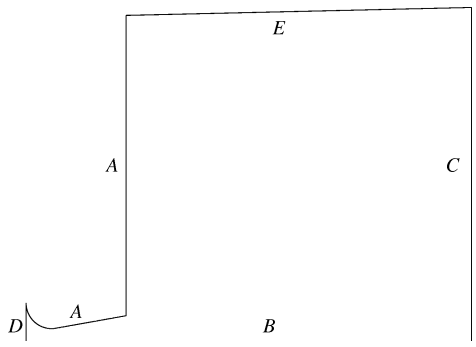

Figure 1: *Boundary conditions*

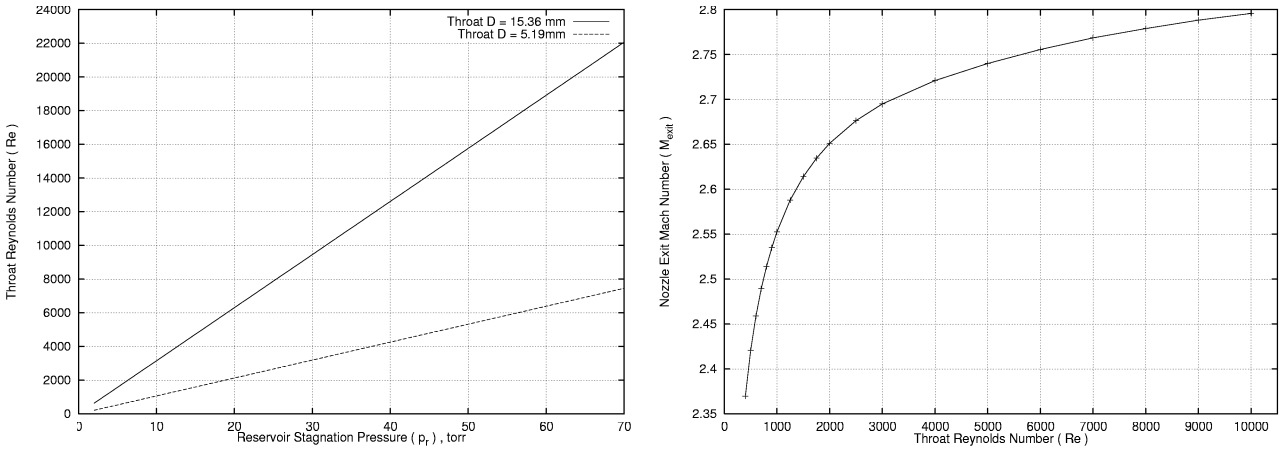

Figure 2: *(a) Reynolds number variation with stagnation pressure (b) Effect of throat Reynolds number on maximum nozzle exit Mach number*

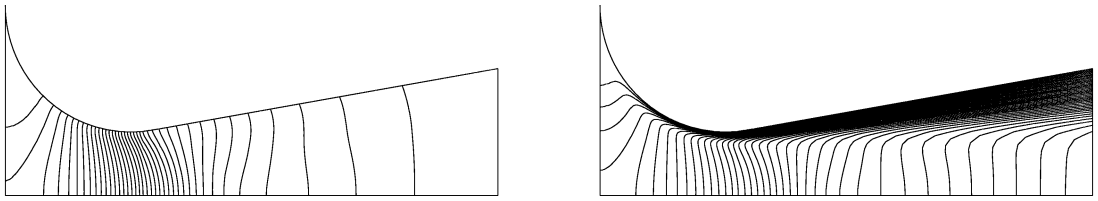

Figure 3: *(a) Pressure contours, nozzle calculation,* Re *= 800.0 (b) Mach number contours, nozzle calculation,* Re *= 800.0*

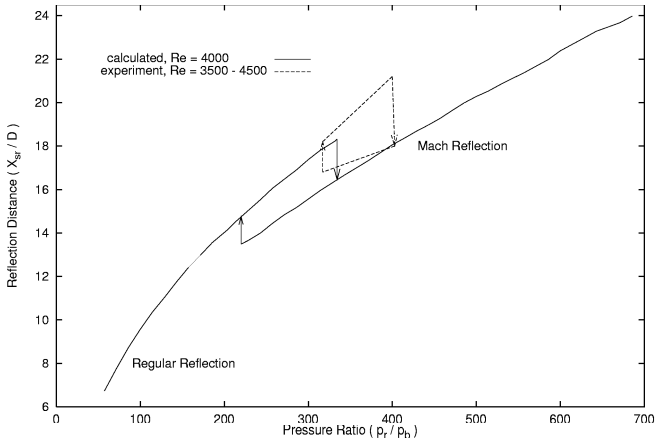

Figure 4: *Reflection distance for range of pressure ratios showing hysteresis loop*

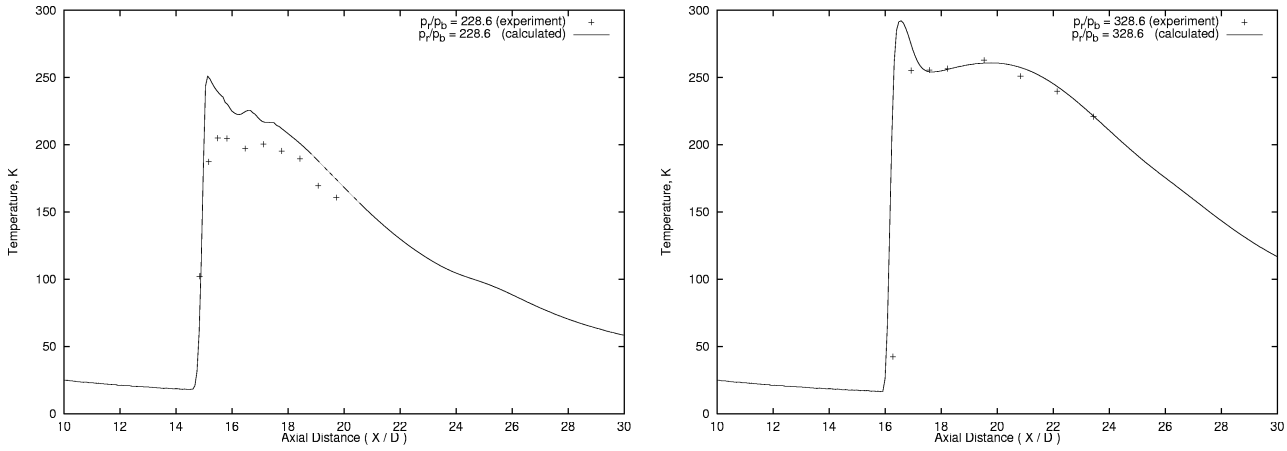

Figure 5: *(a) Centre-line temperature, regular reflection (b) Centre-line temperature, Mach reflection*

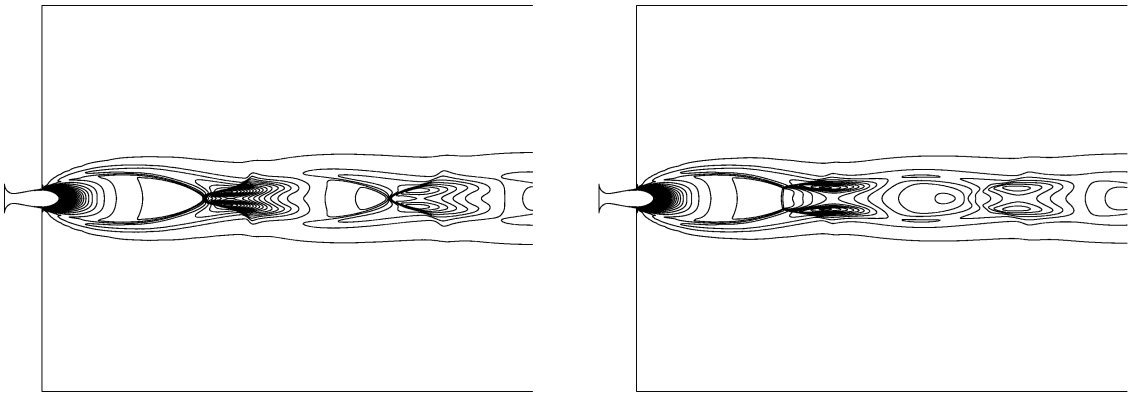

Figure 6: *(a) Density contours showing regular reflection, $p_r/p_b = 285.7$ (b) Density contours showing Mach reflection, $p_r/p_b = 285.7$*

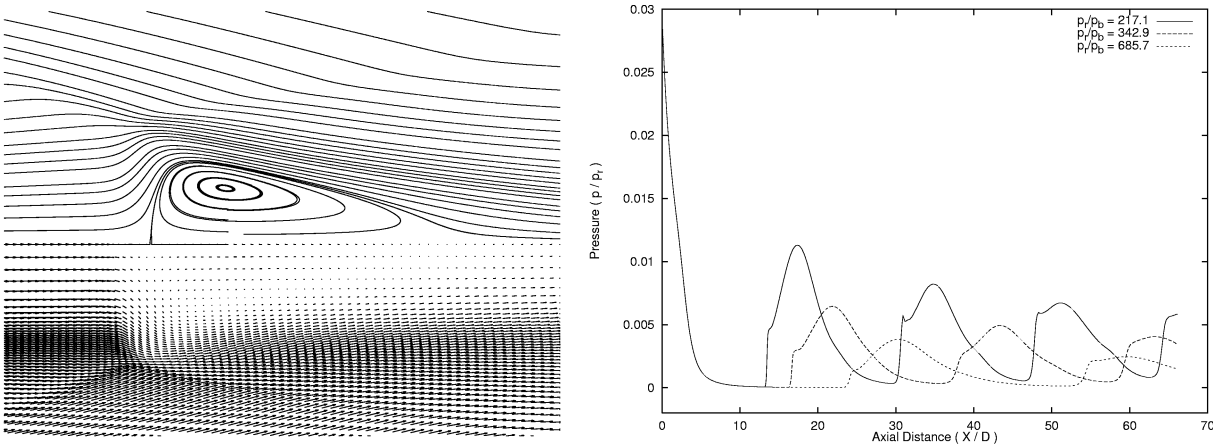

Figure 7: *(a) Velocity vectors and streamlines showing Mach reflection, $p_r/p_b = 342.9$ (b) Centre-line pressure, Mach reflection*